Supporting information

The exposed hematite surface and the generation of environmentally persistent free radicals during catechol degradation

Ziyu Zhao[a], Quan Chen[a], Hao Li[a], Di Lang[a], Meixuan Wu[a], Dandan Zhou[a], Bo Pan[a,]*, Baoshan Xing[b]

[a] Yunnan Provincial Key Laboratory of Soil Carbon Sequestration and Pollution Control, Faculty of Environmental Science & Engineering, Kunming University of Science & Technology, Kunming, 650500, Yunnan, China

[b] Stockbridge School of Agriculture, University of Massachusetts, Amherst, MA 01003, United States

*Corresponding author: Faculty of Environmental Science & Engineering, Kunming University of Science & Technology, Kunming, China, 650500

E-mail address: panbocai@gmail.com (Bo Pan), Phone/Fax: 86-871-65170906

Table S1 The surface areas and porous structures of particles

Type of particles	N_2-BET (m^2/g)	Total pore volume (cm^3/g)	Average pore diameter (nm)
Pure nano hematite	126	0.42	10.92
Pure micro hematite	5	0.01	9.93
Pure silica	341	0.89	7.39
NanoHMT-silica	363	0.87	6.58
MicronHMT-silica	347	0.86	7.08

Table S2 Surface elemental analysis of the investigated particles using XPS

	Sample	C	N	O	Si	Fe	Fe(II)	Fe(III)	Fe(II)%	Fe(III)%
Before reaction	Silica	3.00	0.34	68.93	27.73	-	-	-	-	-
	NanoHMT	6.40	0.69	64.17	19.94	8.80	-	8.80	-	100
	MicroHMT	3.41	0.00	68.14	26.23	2.22	-	2.22	-	100
After reaction	Silica	1.89	0.06	69.43	28.62	-	-	-	-	-
	NanoHMT	5.21	0.91	65.26	23.59	5.02	1.97	3.05	39.24	60.76
	MicroHMT	3.52	0.30	68.16	26.52	1.50	0.46	1.04	30.67	69.33

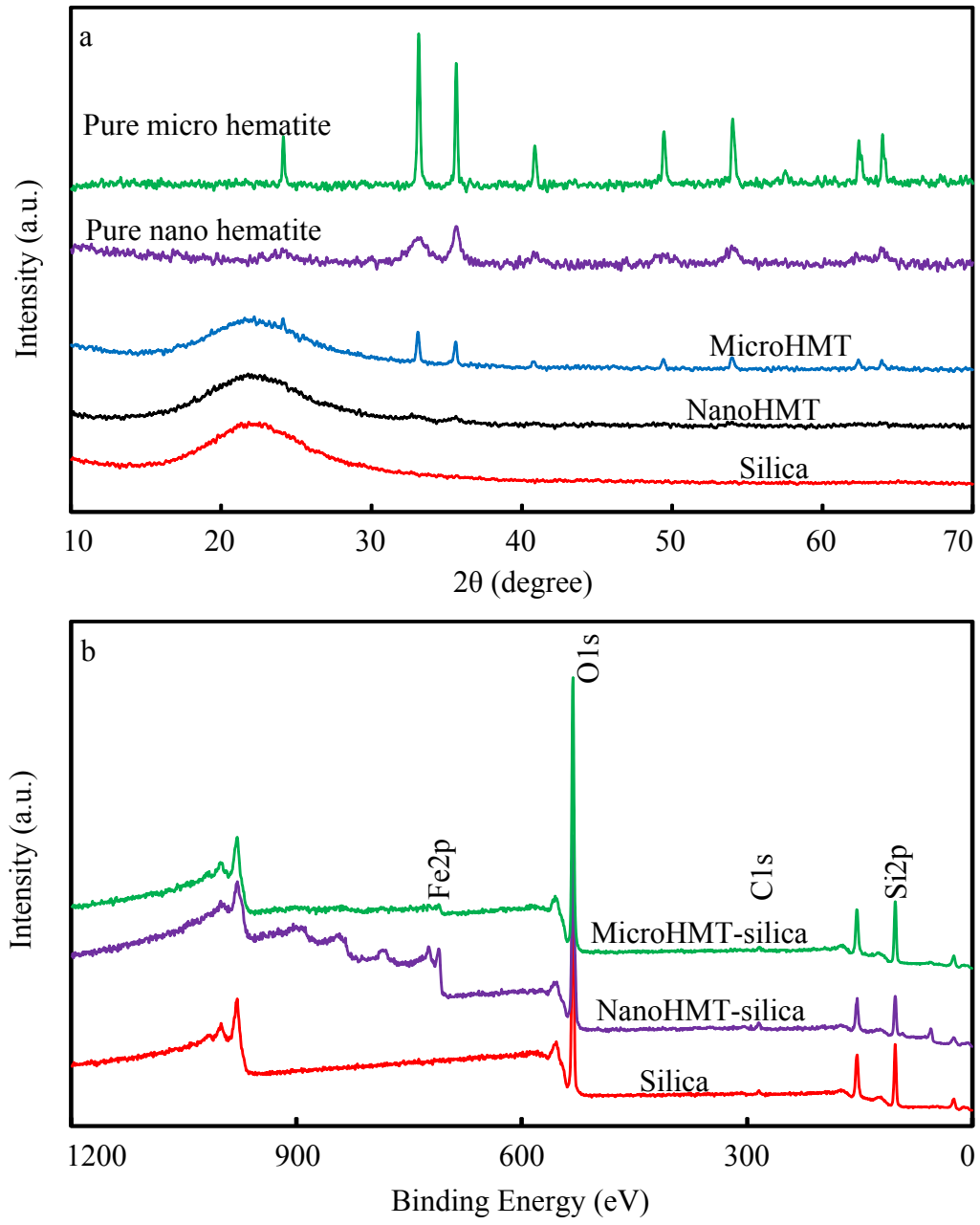

Fig. S1 XRD patterns (a) and surface compositions (b) of silica, nanoHMT, microHMT as well as the pure nano and micro hematites. The surface elemental compositions were analyzed using X-ray photoelectron spectroscopy.

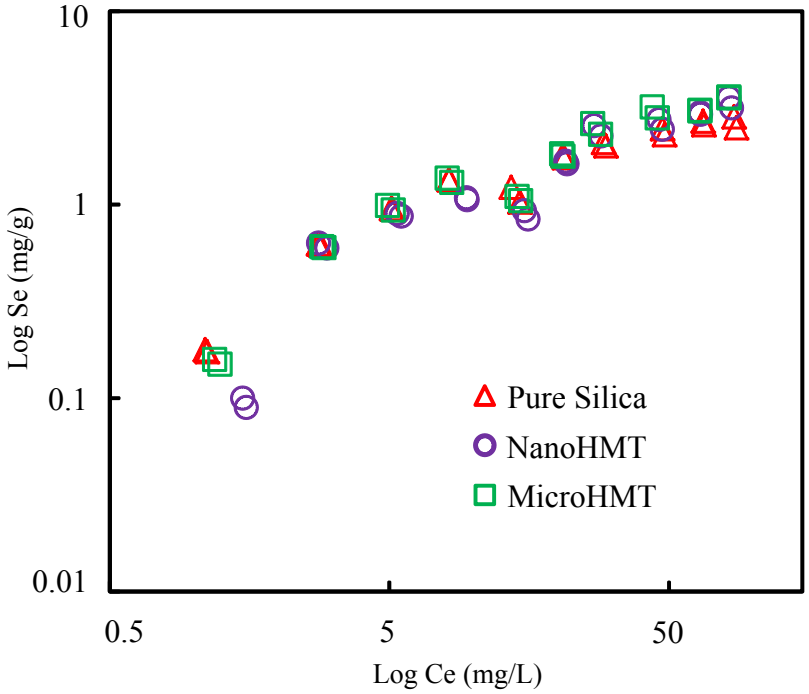

Fig. S2 Adsorption isotherms of catechol on pure silica, nanoHMT, and microHMT.

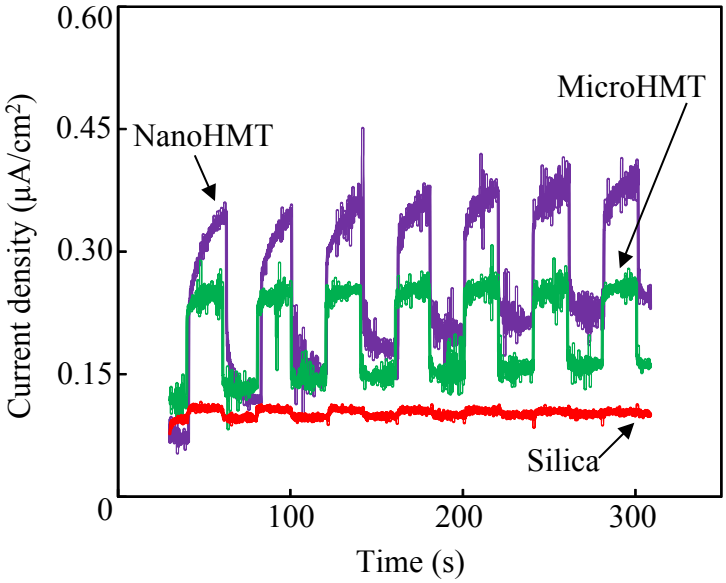

Fig. S3 The photocurrent density of pure silica, nanoHMT and microHMT.

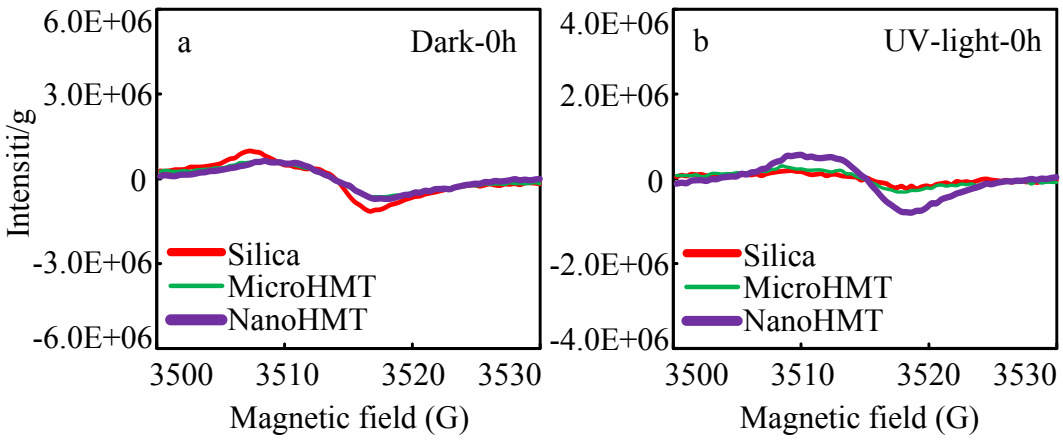

Fig. S4 The EPR signals detected at beginning in the dark (a) and under continuous UV irradiation (b).

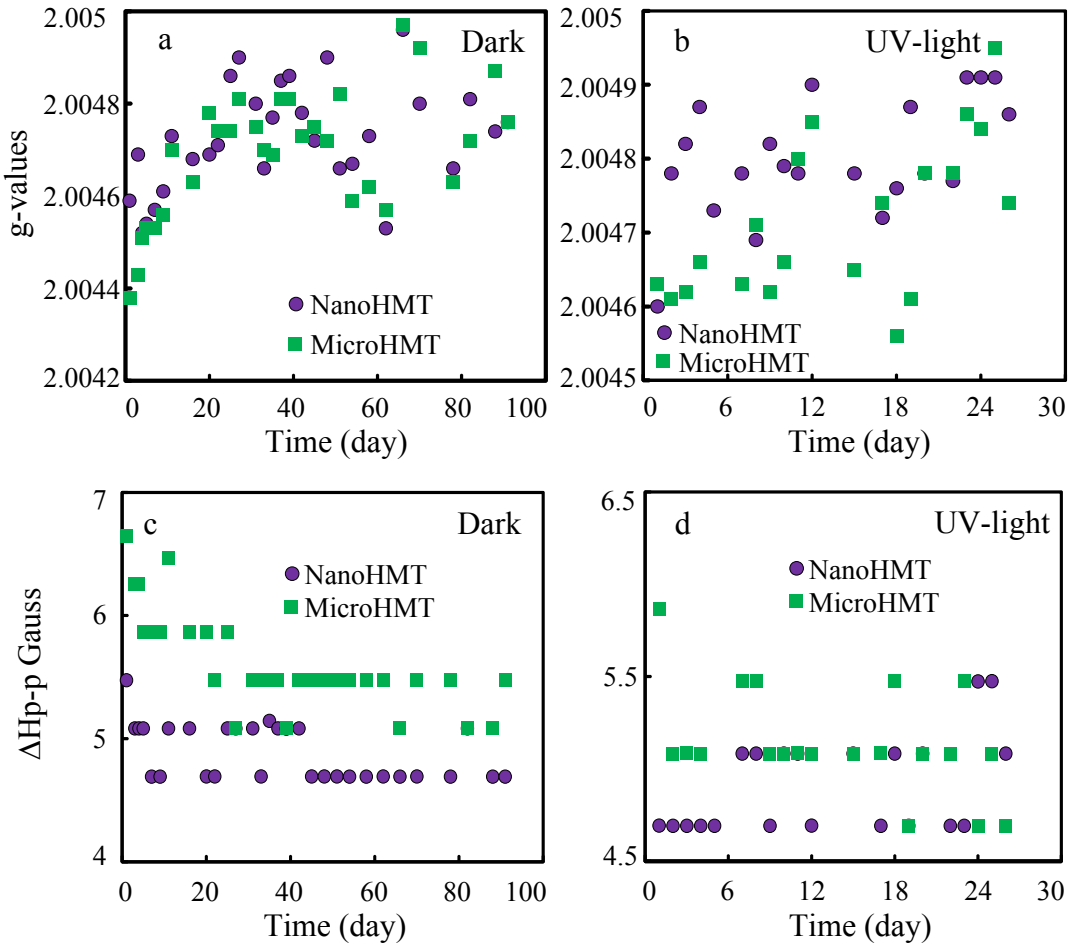

Fig. S5 The g-values (a and b) and the $\Delta H_{P\text{-}P}$ (c and d) of EPFRs variation with time in the dark and under UV irradiation at solid-phase catechol concentrations of 0.60±0.09 μg/mg.

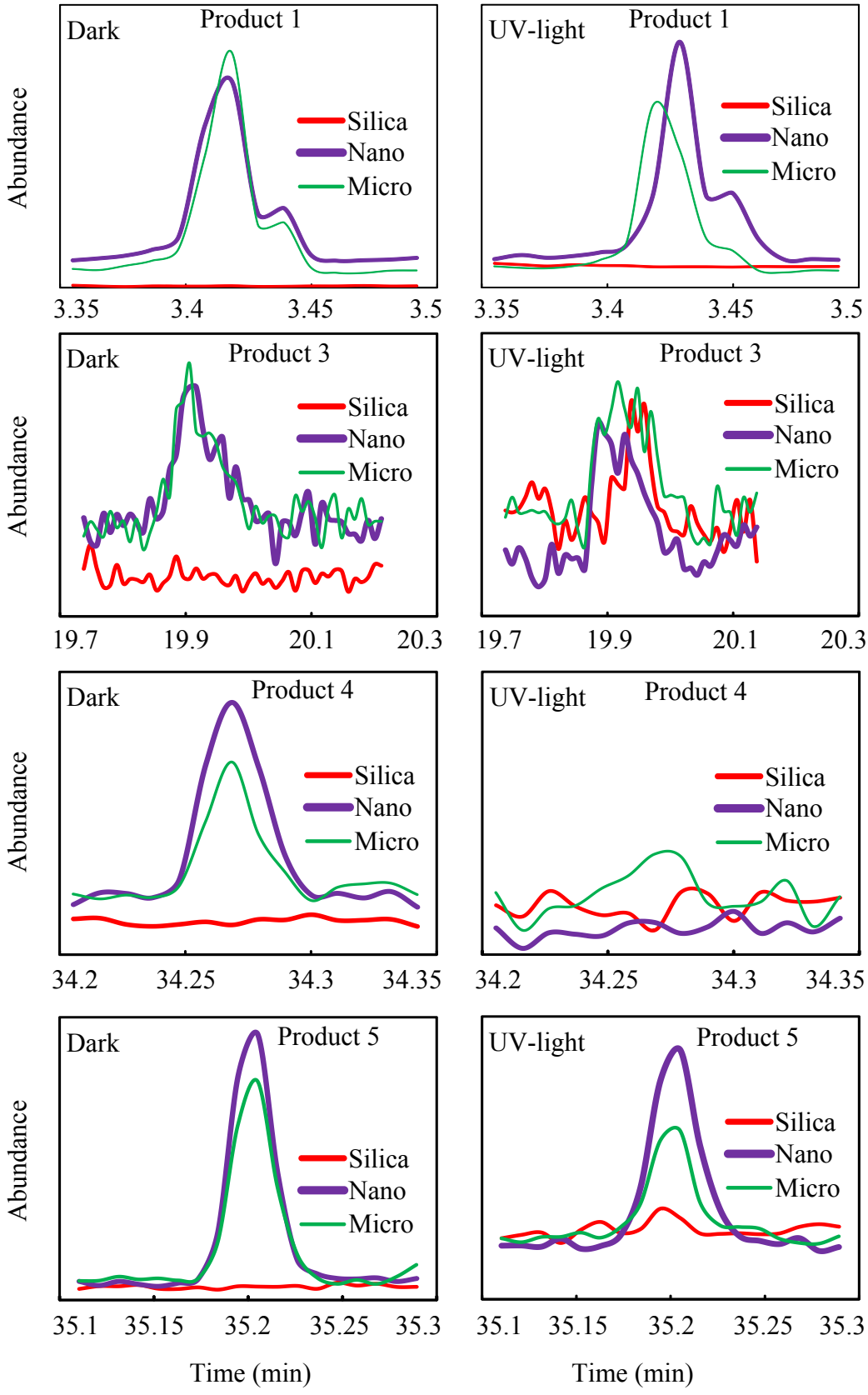

Fig. S6 Comparison of the abundance of main degradation products of catechol in particles under dark and ultraviolet light conditions.

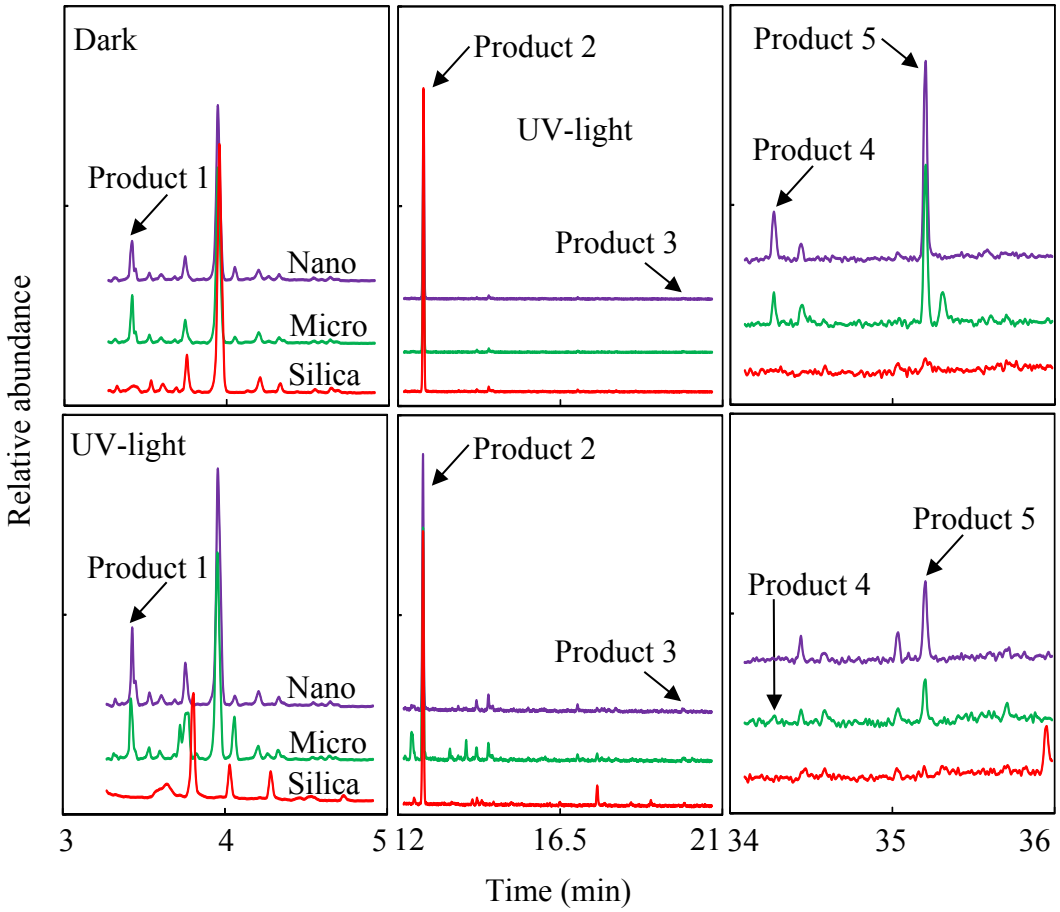

Fig. S7 The GC chromatogram of the degradation products of catechol in particles under dark and ultraviolet light conditions.